

AFRL-SN-HS-TR- 2002-011

**STATISTICAL ANALYSIS OF THE NONHOMOGENIETY DETECTOR FOR
STAP APPLICATIONS**

Dr. Muralidhar Rangaswamy/SNHE

Dr. James Michels/SNRT

Dr. Braham Himed/SNRT

INHOUSE REPORT

NOVEMBER 2001

APPROVED FOR PUBLIC RELEASE: DISTRIBUTION UNLIMITED



**AIR FORCE RESEARCH LABORATORY
Sensors Directorate
80 Scott Dr
Hanscom AFB MA 01731-2909**

20021212 036

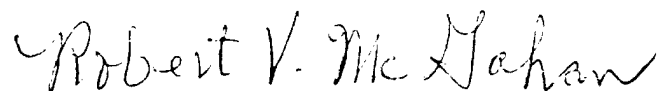
IN HOUSE REPORT

Title: Statistical Analysis of the Nonhomogeneity Detector of STAP Applications

PUBLICATION REVIEW

This report has been reviewed and is approved for publication:

APPROVED:



ROBERT V. MCGAHAN
Technical Advisor
Electronics Technology Division

APPROVED/DISAPPROVED.



RICHARD PAYNE
Division Chief
Electromagnetics Technology Division
AFRL/SNH

REPORT DOCUMENTATION PAGE

Form Approved
OMB No. 0704-0188

The public reporting burden for this collection of information is estimated to average 1 hour per response, including the time for reviewing instructions, searching existing data sources, gathering and maintaining the data needed, and completing and reviewing the collection of information. Send comments regarding this burden estimate or any other aspect of this collection of information, including suggestions for reducing the burden, to Department of Defense, Washington Headquarters Services, Directorate for Information Operations and Reports (0704-0188), 1215 Jefferson Davis Highway, Suite 1204, Arlington, VA 22202-4302. Respondents should be aware that notwithstanding any other provision of law, no person shall be subject to any penalty for failing to comply with a collection of information if it does not display a currently valid OMB control number.

PLEASE DO NOT RETURN YOUR FORM TO THE ABOVE ADDRESS.

1. REPORT DATE (DD-MM-YYYY)	2. REPORT TYPE	3. DATES COVERED (From - To)		
	In-house			
4. TITLE AND SUBTITLE		5a. CONTRACT NUMBER		
		N/A		
		5b. GRANT NUMBER		
6. AUTHOR(S)		N/A		
		5c. PROGRAM ELEMENT NUMBER		
		62204F		
		5d. PROJECT NUMBER		
		4619		
		5e. TASK NUMBER		
		HE		
		5f. WORK UNIT NUMBER		
		4619HE01		
7. PERFORMING ORGANIZATION NAME(S) AND ADDRESS(ES)			8. PERFORMING ORGANIZATION REPORT NUMBER	
AFRL/SNHE 80 Scott Drive Hanscom AFB MA 01731			AFRL-SN-HS-TR-2002-011	
9. SPONSORING/MONITORING AGENCY NAME(S) AND ADDRESS(ES)			10. SPONSOR/MONITOR'S ACRONYM(S)	
			11. SPONSOR/MONITOR'S REPORT NUMBER(S)	
12. DISTRIBUTION/AVAILABILITY STATEMENT				
APPROVED FOR PUBLIC RELEASE: DISTRIBUTION UNLIMITED. ESC-01-1438				
13. SUPPLEMENTARY NOTES				
14. ABSTRACT We present a statistical analysis of the recently proposed non-homogeneity detector (NHD) for Gaussian interference statistics. We show that a formal goodness-of-fit test can be constructed by accounting for the statistics of the generalized inner product (GIP) used as the NHD test statistic. Specifically, the Normalized-GIP is shown to follow a central-F distribution and admits a canonical representation in terms of two statistically independent Chi-squared distributed random variables. Moments of the GIP can be readily calculated as a result. These facts are used to derive the goodness-of-fit tests, which facilitate intelligent training data selection. Additionally, we address the issue of space-time adaptive processing (STAP) algorithm performance using the NHD as a pre-processing step for training data selection. Performance results for the adaptive matched filter (AMF) method are reported using simulated as well as measured data.				
15. SUBJECT TERMS STAP, Training Data, Non-homogeneity Detector, Chi-Squared Distribution, Central-F Distribution, Goodness-of-fit Test, MCARM Data, Probability of false alarm (Pfa), Probability of Detection (Pd), Signal-to-Interference Plus Noise-Ratio (SINR), AMF				
16. SECURITY CLASSIFICATION OF:		17. LIMITATION OF ABSTRACT	18. NUMBER OF PAGES	19a. NAME OF RESPONSIBLE PERSON
a. REPORT UNCLAS	b. ABSTRACT UNCLAS	c. THIS PAGE UNCLAS	UNC	Dr. Muralidhar Rangaswamy
19b. TELEPHONE NUMBER (Include area code) (781) 377-3446				

ABSTRACT (CONTINUED FROM SF 298)

The results of some preliminary measurements, made at X-band, of the radar cross section (RCS) and images of model trees that scale to 235 to 355 MHz in the VHF-UHF bands are presented. We designed the model trees to match the growth patterns of forest trees and matched the dielectric properties of the model tree and ground plane materials to live softwood tree wood and moist soil. The dimensional and angle accuracy of the model trees, fabricated from CAD files we generated, were very high, $\lambda/50$ and 1 deg, respectively. A newly developed method-of-moments RCS prediction code will be used to compute the full-size version of the model tree's RCS and compare it to the model measurements. We measured the models in free space and on ground planes to reveal the fundamental scattering phenomena of *in situ* trees.

Preliminary results show that the roots have negligible impact on the overall RCS of a tree because of the transmission loss into and out of the soil and the attenuation of the wave propagating in the soil. Also, the dominant scattering mechanism is the dihedral multipath effect that increases the *in situ* RCS of the tree trunk to nearly its broadside value. The contributions from the branches interfere with one another and that of the trunk to produce an RCS scattering pattern that varies as the aspect angle varies. Prominent variations in the RCS of the trunk occur with changes in frequency. Their impact on the RCS diminishes as the number of branches increases.

In the next phase of the program, scaled measurements will be made down to 100 MHz at grazing angles from 20 – 60 degrees, new trees and larger ground planes will be fabricated to model different dielectric constants and tree species, and the measurement system will be made fully polarimetric.

VHF/UHF scale-model measurements are a powerful new research tool to collect, quickly and cost effectively, data to evaluate competing operational scenarios and to assess the efficacy of various signal and image processing techniques that reduce false alarms and discriminate target signals from tree clutter. The application of this technique will help to show whether certain approaches or radar operating parameters would or would not improve performance. This would help to focus full-scale measurements to specific areas that need further investigation thereby saving the resources required to field potentially unnecessary full-scale foliage penetration SAR experiments or system development.

Preface

The authors would like to thank Thomas Horgan and Tatal Chouman of the Submillimeter-Wave Technology Laboratory for construction of the scale model trees used in this research and Chris Beaudoin for assisting with the model measurements. A portion of this work was supported by the National Ground Intelligence Center, Charlottesville, VA under contract #DASC01-01-C-0011.

Executive Summary

We present a statistical analysis of the recently proposed non-homogeneity detector (NHD) for Gaussian interference statistics in this report. We show that a formal goodness-of-fit test can be constructed by accounting for the statistics of the generalized inner product (GIP) used as the NHD test statistic. Specifically, the Normalized-GIP is shown to follow a central-F distribution and admits a canonical representation in terms of two statistically independent Chi-squared distributed random variables. Moments of the GIP can be readily calculated as a result. These facts are used to derive the goodness-of-fit tests, which facilitate intelligent training data selection. Additionally, we address the issue of space-time adaptive processing (STAP) algorithm performance using the NHD as a pre-processing step for training data selection. Performance results for the adaptive matched filter (AMF) method are reported using simulated as well as measured data.

Contents

1	Introduction	1
2	GIP Statistics: Known Covariance	3
3	GIP Statistics: Unknown Covariance	5
4	New Test for Nonhomogeneity	7
5	Performance Analysis of the Non-Homogeneity Detector	8
6	Performance Analysis of the AMF Test	14
7	Conclusion	21

List of Figures

5.1	PDF of the normalized GIP	9
5.2	Theoretical and empirical CDF of the normalized GIP	10
5.3	Type-I error versus threshold	11
5.4	Normalized GIP vs Range	12
5.5	Normalized GIP vs Range	13
6.1	AMF test Performance: P_d versus SINR	16
6.2	Normalized GIP vs Range	17
6.3	Absolute value of difference between GIP and Theoretical GIP mean vs Range	18
6.4	AMF Test Statistic versus Range	19

Chapter 1

Introduction

An important issue in space-time adaptive processing (STAP) for radar target detection is the formation and inversion of the covariance matrix underlying the clutter/interference. In practice, the unknown interference covariance matrix is estimated from a set of independent identically distributed (iid) target-free training data which is assumed to be representative of the interference statistics in a cell under test. Frequently, the training data is subject to contamination by discrete scatterers or interfering targets. In either event, the training data becomes nonhomogeneous. As a result, it is non representative of the interference in the test cell. Estimates of the covariance matrix from nonhomogeneous training data result in severely undernulled clutter. Consequently, CFAR and detection performance suffer. Significant performance improvement can be achieved by employing pre-processing to select representative training data.

The problem of target detection using improved training strategies has been considered in [1–8]. The impact of nonhomogeneity on STAP performance is considered in [8–11]. It was shown in [12] that the distribution information of a class of multivariate probability density functions (PDF) is succinctly determined through an equivalent univariate PDF of a quadratic form. An application of this result is the non-homogeneity detector (NHD) based on the generalized inner product (GIP) [1–4, 8, 13].

Non-homogeneity of the training data arises due to a number of factors such as contaminating targets, presence of strong discretes, and non-stationary reflectivity properties of the scattering surface. In these scenarios, the test cell disturbance covariance matrix, $\hat{\mathbf{R}}_T$, differs significantly from the estimated covariance matrix, $\hat{\mathbf{R}}$, formed using target-free disturbance realizations from adjacent reference cells. If a large number of test cell data realizations are available, the underlying non-homogeneity is characterized via the eigenvalues of $\hat{\mathbf{R}}^{-1}\hat{\mathbf{R}}_T$ [13]. However, in radar applications, only a single realization of test cell data is usually available. Consequently, the resulting estimate, $\hat{\mathbf{R}}_T$, is singular. Hence, the works of [1–4, 8, 13] have addressed the use of a non-homogeneity detector (NHD) which compares an empirically formed GIP with a theoretically calculated mean based on the known covariance matrix. Large deviations of the GIP mean from the theoretical mean have been ascribed to non-homogeneity of the training data. Such an approach provides meaningful results in the limit of large training data size. In practice, the amount

of training data available for a given application is limited by system considerations such as bandwidth and fast scanning arrays. Furthermore, the inherent temporal and spatial non-stationarity of the interference precludes the collection of large amounts of training data. Consequently, the approach of [1–4, 8, 13] can be misleading since it ignores finite data effects and the resulting variability in the covariance matrix estimate.

In this report we derive significant results pertaining to the statistics of the GIP for Gaussian interference. In particular, our results reveal that the empirical GIP mean using an estimated covariance matrix with finite data can be twice as large as the corresponding GIP mean for a known covariance matrix. Consequently, such a scenario can easily lead to incorrect classification of training data. The main result of this report is that the normalized GIP, P' , admits a remarkably simple stochastic representation as the ratio of two statistically independent Chi-Squared distributed random variables. As a result, the GIP follows a central-F distribution. The stochastic representation facilitates rapid calculation of the GIP moments. These facts are exploited to construct a formal goodness-of-fit test for selecting homogeneous training data.

We also present performance analyses of the NHD using the goodness-of-fit test for the GIP. Performance results are presented using both simulated and measured data. We then employ the NHD as a pre-processing step for training data selection and assess performance of the adaptive matched filter (AMF) test [14–16]. Performance is reported in terms of the probability of detection versus output signal to noise ratio for simulated data. For measured data, a plot of the test statistic versus range is used as a performance metric.

Chapter 2

GIP Statistics: Known Covariance

Let $\mathbf{x} = [x_1 \ x_2 \ \dots \ x_M]^T$ denote a complex random vector with zero mean and known positive definite Hermitian covariance matrix \mathbf{R} . The quadratic form given by $Q = \mathbf{x}^H \mathbf{R}^{-1} \mathbf{x}$ has the important property that $E(Q) = M$ [17]. This result is readily proven below.

$$Q = \mathbf{x}^H \mathbf{R}^{-1} \mathbf{x} = \text{tr}[\mathbf{x}^H \mathbf{R}^{-1} \mathbf{x}] = \text{tr}[\mathbf{R}^{-1} \mathbf{x} \mathbf{x}^H] \quad (2.1)$$

where $\text{tr}(.)$ denotes the trace of a matrix. We have made use of the fact that $\text{tr}(\mathbf{AB}) = \text{tr}(\mathbf{BA})$. Hence,

$$\begin{aligned} E(Q) &= E\{\text{tr}[\mathbf{R}^{-1} \mathbf{x} \mathbf{x}^H]\} = \text{tr}[\mathbf{R}^{-1} E\{\mathbf{x} \mathbf{x}^H\}] \\ &= \text{tr}(\mathbf{R}^{-1} \mathbf{R}) = \text{tr}(\mathbf{I}_M) = M \end{aligned} \quad (2.2)$$

where \mathbf{I}_M is the $M \times M$ identity matrix. This result is important in that it is independent of the PDF underlying \mathbf{x} and is only a function of the dimension of the random vector.

If the PDF of \mathbf{x} is known, the corresponding PDF of Q can be readily derived. For Gaussian distributed \mathbf{x} , i.e., $\mathbf{x} \sim CN(0, \mathbf{R})$, the PDF of Q is a Chi-Squared distribution with M complex degrees of freedom. More precisely,

$$Q = \mathbf{x}^H \mathbf{R}^{-1} \mathbf{x} = \|\mathbf{R}^{-\frac{1}{2}} \mathbf{x}\|^2 \quad (2.3)$$

where $\|.\|$ denotes the Euclidean vector norm. Letting $\mathbf{y} = \mathbf{R}^{-\frac{1}{2}} \mathbf{x}$ gives

$$Q = \|\mathbf{y}\|^2 = \sum_{i=1}^M |Y_i|^2 \quad (2.4)$$

where Y_i , $i = 1, 2, \dots, M$ are iid $CN(0, 1)$ random variables. Since Q is the sum of the squared magnitudes of M iid $CN(0, 1)$ random variables, it follows that Q is a Chi-Squared distributed random variable with M complex degrees of freedom [17]. The PDF of Q is given by

$$f_Q(q) = \frac{q^{M-1}}{\Gamma(M)} \exp(-q) \quad 0 \leq q < \infty \quad (2.5)$$

where $\Gamma(.)$ is the Euler-Gamma function. The PDF of Q is derived in Appendix A.

The GIP based NHD calculates the quadratic form Q using an estimated covariance matrix (formed from iid target free training data) and compares its mean with the dimensionality of the random vector \mathbf{x} . Deviations from M have been attributed to non-homogeneities in the training data [1–4,8]. In practice, the interference covariance matrix is formed from a finite amount of training data. The statistical variability associated with the data could introduce additional errors and thus deviations of the GIP from M cannot entirely be ascribed to the presence of non-homogeneities. Consequently, it is useful to work with the statistics of Q formed with an estimated covariance matrix.

Chapter 3

GIP Statistics: Unknown Covariance

The complex-Gaussian test data vector is denoted by $\mathbf{x} \sim CN(0, \mathbf{R}_T)$, where \mathbf{R}_T is unknown. Let \mathbf{z}_i , $i = 1, 2, \dots, K$ denote iid $CN(0, \mathbf{R}_z)$ target free training data. For representative (homogeneous) training data, $\mathbf{R}_T = \mathbf{R}_z = \mathbf{R}$. The maximum likelihood estimate of the covariance matrix is given by

$$\hat{\mathbf{R}} = \frac{1}{K} \sum_{i=1}^K \mathbf{z}_i \mathbf{z}_i^H. \quad (3.1)$$

Let $P = \mathbf{x}^H \hat{\mathbf{R}}^{-1} \mathbf{x}$. A stochastic representation for the normalized GIP denoted by $P' = \frac{P}{K}$ is derived in Appendix B. Consequently, P can be expressed as

$$P = \frac{KR_1}{R_2} \quad (3.2)$$

where R_1 and R_2 are statistically independent Chi-squared distributed random variables with PDFs given by

$$f_{R_1}(r_1) = \frac{r_1^{M-1}}{\Gamma(M)} \exp(-r_1) \quad 0 \leq r_1 < \infty \quad (3.3)$$

$$f_{R_2}(r_2) = \frac{r_2^{K-M}}{\Gamma(K-M+1)} \exp(-r_2) \quad 0 \leq r_2 < \infty \quad (3.4)$$

respectively. The PDF of P' , which is simply a central-F distribution [18], is expressed as

$$f_{P'}(r) = \frac{1}{\beta(L, M)} \frac{r^{M-1}}{(1+r)^{M+L}} \quad 0 \leq r < \infty \quad (3.5)$$

where $L = K - M + 1$ and

$$\beta(m, n) = \int_0^1 \theta^{m-1} (1-\theta)^{n-1} d\theta. \quad (3.6)$$

The statistical equivalence of P to within a scalar of the ratio of two independent chi-square distributed random variables is fascinating in that it permits rapid calculation of the moments of P . More importantly, it is extremely useful in Monte-Carlo studies involving computer generation of P . For homogeneous training data, the use of (3.2) circumvents the need to explicitly generate the test data vector \mathbf{x} and the training data vectors used for covariance estimation. For large M and perforce K , significant computational savings can be realized from the method of (3.2).

It can be readily shown that

$$\begin{aligned} E(P) &= KE(R_1)E(R_2^{-1}) = \frac{M}{[1 - \frac{M}{K}]} \\ \sigma_P^2 &= \frac{M}{\left[1 - \frac{M}{K}\right]\left[1 - \frac{(M+1)}{K}\right]} \end{aligned} \quad (3.7)$$

where $E(P)$ and σ_P^2 denote the mean and variance of P , respectively. We then consider the PDF of $\frac{R_2}{K}$ in the limit of large K . The characteristic function of $\frac{R_2}{K}$ is given by

$$\Phi_{R_2}(j\omega) = E[\exp(-j\omega \frac{R_2}{K})] = \frac{1}{(1 + \frac{j\omega}{K})^{K-M+1}}. \quad (3.8)$$

In the limit of $K \rightarrow \infty$, we have

$$\Psi(j\omega) = \lim_{K \rightarrow \infty} \Phi_{R_2}(j\omega) = \exp(-j\omega). \quad (3.9)$$

The PDF of $\frac{R_2}{K}$ in the limit of $K \rightarrow \infty$ is given by

$$f_{R_2}(r) = \frac{1}{2\pi} \int_{-\infty}^{\infty} \exp[(r-1)j\omega] d\omega = \delta(r-1). \quad (3.10)$$

Hence, for $K \rightarrow \infty$, R_2/K becomes unity with probability 1. Consequently, the GIP is simply R_1 and hence, follows a Chi-Squared distribution with M complex degrees of freedom. Thus for $K \rightarrow \infty$, $E(P) = M$ and $\sigma_P^2 = M$, corresponding to the known covariance matrix results. Consequently, the GIP statistical representation given by (3.2) provides additional insights into the NHD. The numerator random variable corresponds to the GIP statistics for known covariance matrix. The denominator random variable succinctly embeds the deleterious effects of estimating the covariance matrix with finite sample support as well as nonhomogeneity of the training data. A manifestation of this effect can be seen from the deviation of the statistics of R_2 from the Chi-Squared distribution.

Chapter 4

New Test for Nonhomogeneity

The work of [1–4,8] uses an NHD based on comparing the mean of empirically formed GIPs (from different realizations of test data) to M . Large deviations from M are ascribed to nonhomogeneities. However, the effects of finite data support and the associated statistical variability can result in large deviations of the empirical GIP mean from M . Thus, a more stringent test for the GIP based NHD consists of the following steps:

1. Form the GIP denoted by P for a given K .
2. Perform a goodness-of-fit test of the empirically formed $\frac{P}{K}$ with the theoretically predicted PDF of (3.5). Specifically, we set the type-I error, α , to be 0.1. This is simply the probability of incorrectly rejecting the hypothesis that the data comes from the F-distribution of (3.5). More precisely, this corresponds to calculating a threshold λ , such that $\alpha = \Pr(P' > \lambda) = 0.1$. From (3.5), it follows that

$$\Pr(P' > \lambda) = \text{betainc}\left(\frac{1}{\lambda + 1}, M, L\right) \quad (4.1)$$

where

$$\text{betainc}(x, M, L) = \frac{1}{\beta(M, L)} \int_0^x \theta^{M-1} (1-\theta)^{L-1} d\theta. \quad (4.2)$$

Given α , M , and L , λ is readily calculated from an inversion of (4.1). The goodness-of-fit test consists of comparing the empirically formed P' from each training data realization with λ and rejecting those realizations for which P' exceeds λ .

3. A second method for the goodness-of-fit test is a comparison of the empirical GIP mean to the theoretically predicted mean value of (3.7) and retaining those GIP realizations, which exhibit the least deviation. Large discrepancies between the theoretical and empirical means result from nonhomogeneities.

The performance of the goodness-of-fit test methods is presented in the next section.

Chapter 5

Performance Analysis of the Non-Homogeneity Detector

We present performance results of our approach here. Figure 5.1 shows the PDF of P' for several values of K with $M=8$ for Gaussian interference statistics. Observe that the variance of P' decreases with increasing K . This is anticipated since $\hat{\mathbf{R}}$ tends to \mathbf{R} with probability 1 as $K \rightarrow \infty$. The results presented in Figures 5.2 and 5.3 correspond to the case of homogeneous training data. Figure 5.2 presents a comparison of the cumulative distribution function (CDF) of P' obtained from Monte-Carlo realizations using simulated data with the theoretically predicted CDF of P' obtained by numerical integration of (3.5). The results show good agreement between the theoretical prediction and the empirically generated values. The mean value of P , 15.957, obtained via Monte-Carlo compares well with the theoretically predicted value of 16. Figure 5.3 plots the type-I error versus threshold for $M=64$. Here different values of K are chosen to illustrate the threshold behavior. For each value of α , λ is determined from a numerical inversion of (4.1). For a given α we observe an increase in λ with increasing K . Examples that illustrate the two goodness-of-fit test approaches are presented. For a given training data set, a moving window approach is used to form realizations of P' . This approach is sub-optimal because it does not guarantee statistical independence of the realizations of P' . However, we adopt this approach due to the limited training data support. For the examples presented in Figures 5.4 and 5.5, data from the MCARM program [19] corresponding to 16 pulses and 8 channels from acquisition '220' on Flight 5, cycle 'e' is used.

Figure 5.4 shows the results of the goodness of fit test for the based on the PDF of P' . The normalized GIP and the threshold are plotted as a function of range. Non-homogeneity of the training data is evident in those bins for which the normalized GIP exceeds the threshold. Figure 5.5 plots the normalized GIP as a function of range. The normalized GIP theoretical mean is obtained from (3.7) with a simple normalization. Values of the normalized GIP, which exceed the theoretical mean correspond to non-homogeneous training data realizations. Observe that this method is more sensitive to the presence of discrete scatterers in the training data.

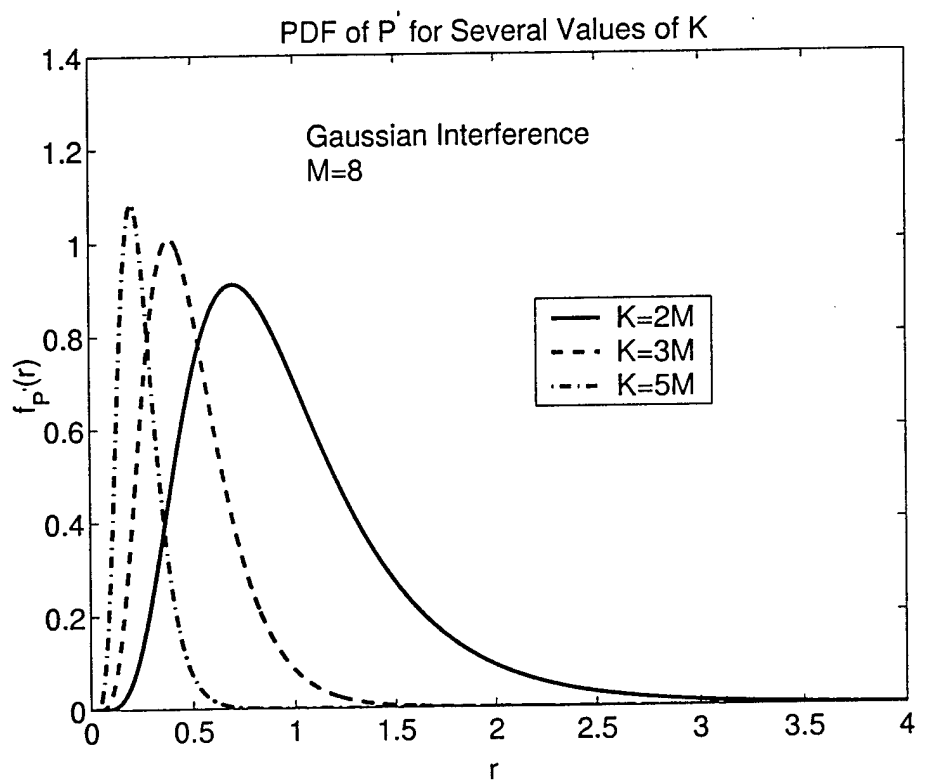


Figure 5.1: PDF of the normalized GIP

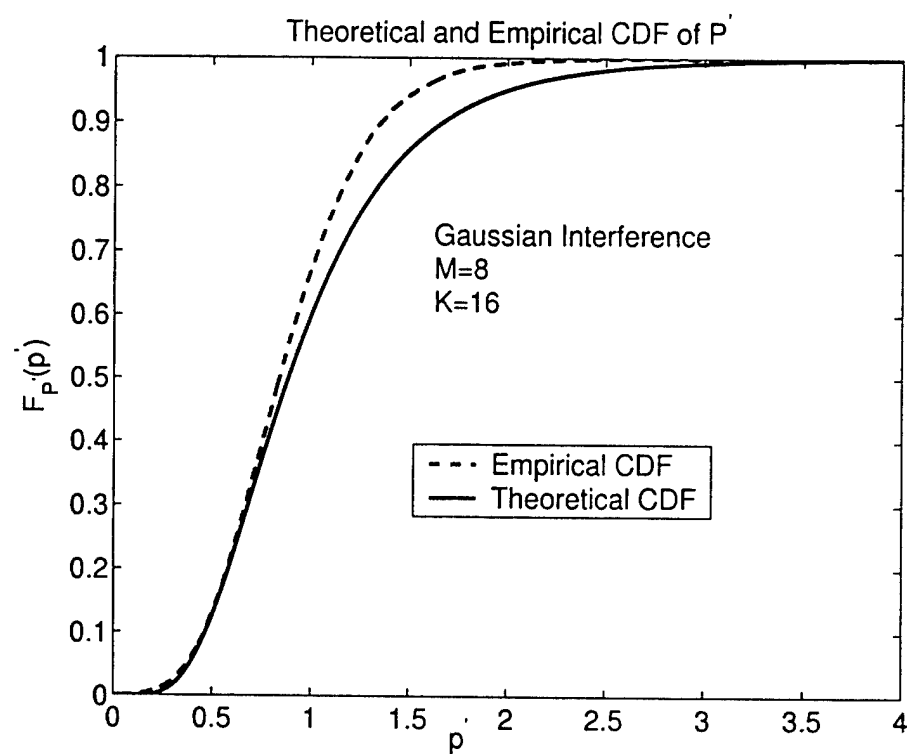


Figure 5.2: Theoretical and empirical CDF of the normalized GIP

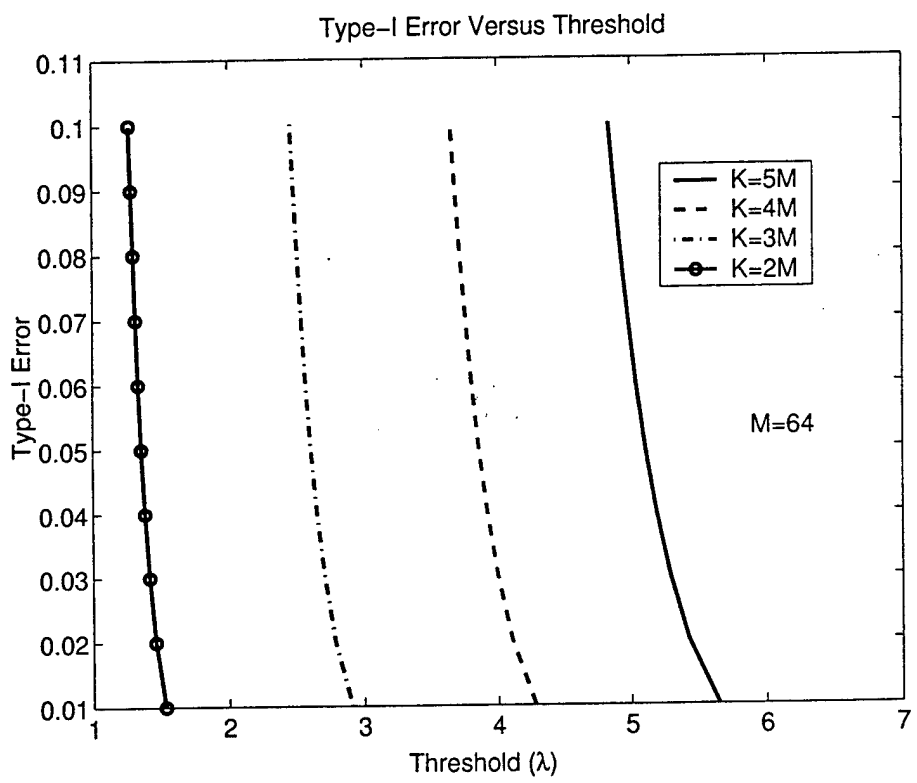


Figure 5.3: Type-I error versus threshold

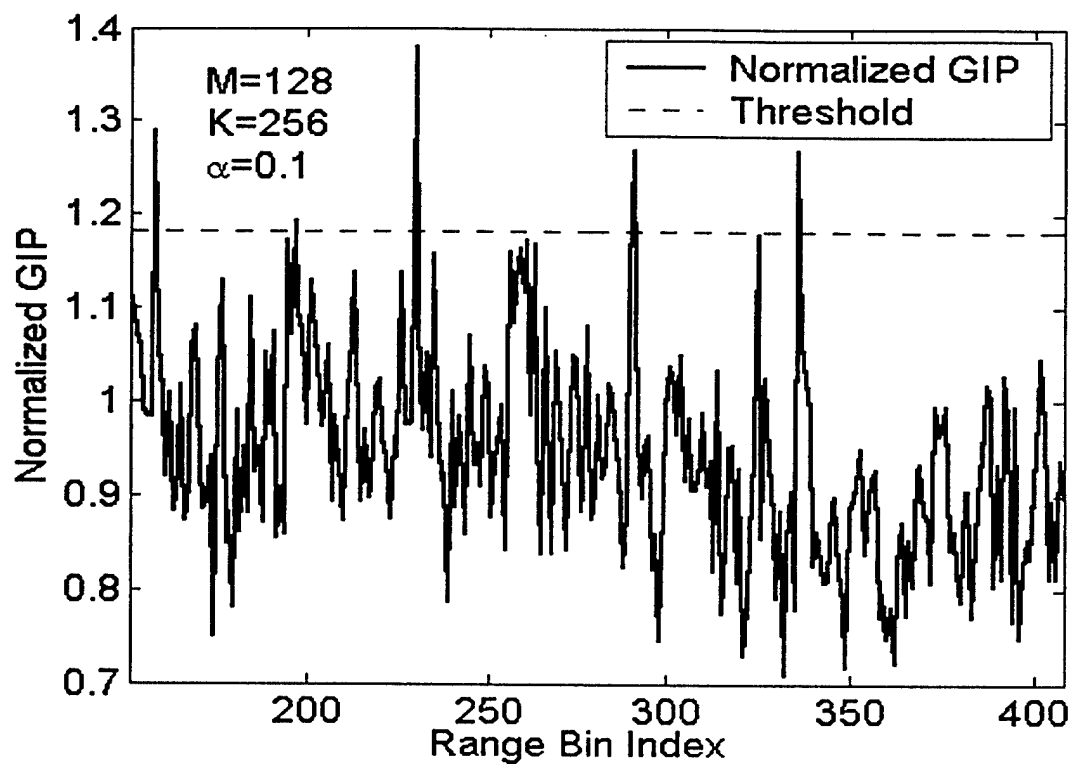


Figure 5.4: Normalized GIP versus Range

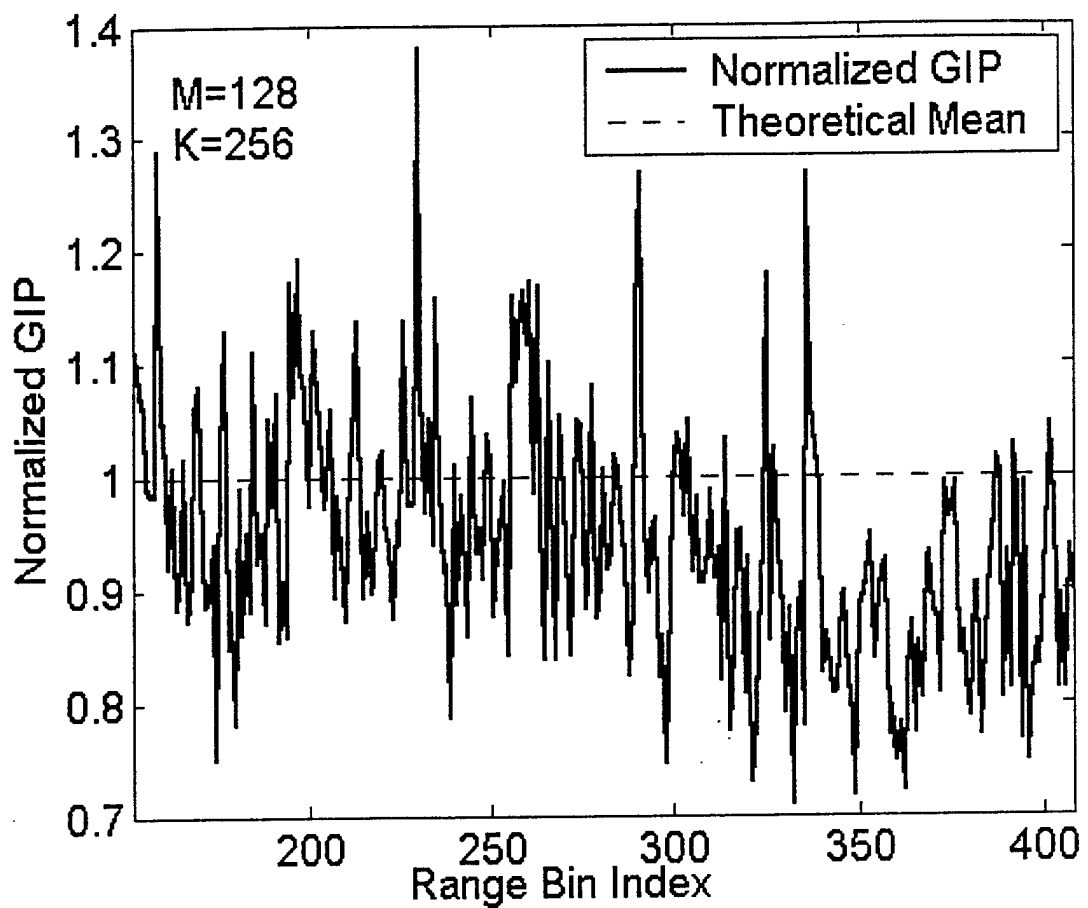


Figure 5.5: Normalized GIP versus Range

Chapter 6

Performance Analysis of the AMF Test

The adaptive matched filter test is given by

$$\Lambda_{AMF} = \frac{|\mathbf{s}^H \hat{\mathbf{R}}_d^{-1} \mathbf{x}|^2}{\mathbf{s}^H \hat{\mathbf{R}}_d^{-1} \mathbf{s}} \stackrel{H_1}{>} \stackrel{H_0}{<} \lambda_{AMF}. \quad (6.1)$$

where $\hat{\mathbf{R}}_d = \frac{1}{K} \sum_{i=1}^K \mathbf{x}_i \mathbf{x}_i^H$, with \mathbf{x}_i , $i = 1, 2, \dots, K$ denoting independent identically distributed target-free training data vectors.

The expressions for P_{fa} and P_d for the AMF operating in homogeneous Gaussian clutter are given by [14–16]

$$P_{fa-AMF} = \int_0^1 \frac{f_\Gamma(\gamma)}{[1 + \text{gamma} \lambda_{AMF}]^L} d\gamma \quad (6.2)$$

$$\begin{aligned} P_{d-AMF} &= 1 - \int_0^1 \frac{1}{[1 + \text{gamma} \lambda_{AMF}]^L} \\ &\times \sum_{m=1}^L \binom{L}{m} \eta^m \gamma^m \\ &\times [1 - \text{gammainc}\left(\frac{A\gamma}{1 + \gamma \lambda_{AMF}}, m\right)] f_\Gamma(\gamma) d\gamma \end{aligned} \quad (6.3)$$

where

$$\Gamma = \frac{1}{[1 + \mathbf{x}^H \hat{\mathbf{R}}_d^{-1} \mathbf{x} / K]} \quad (6.4)$$

is the well known loss-factor with PDF [20]

$$f_\Gamma(\gamma) = \frac{1}{\beta(L+1, JN-1)} \gamma^L (1-\gamma)^{JN-2} \quad (6.5)$$

where $L = K - JN + 1$, A is related to the output signal-to-noise-ratio and $\text{gammainc}(p, m)$ is defined as

$$\text{gammainc}(p, m) = \frac{1}{\Gamma(m)} \int_0^p \theta^{m-1} \exp(-\theta) d\theta. \quad (6.6)$$

For $K \rightarrow \infty$, $\hat{\mathbf{R}}_d \rightarrow \mathbf{R}_d$ with probability 1. Thus, the expressions for AMF P_{fa} and P_d approach those of the matched filter, given by

$$\begin{aligned} P_{fa} &= \exp(-\lambda_{MF}) \\ P_d &= \exp(-B) \sum_{k=0}^{\infty} \frac{A^k}{k!} [1 - \text{gammaintc}(\lambda_{MF}, k)] \end{aligned} \quad (6.7)$$

Figure 6.1 presents P_d versus output signal-to-interference plus noise ratio (SINR). Relevant test parameters are reported in the plot. The matched filter (MF) curve obtained from (6.7) corresponds to the optimal performance in Gaussian clutter. The P_d curve for the AMF operating in homogeneous Gaussian clutter follows from (6.3) and exhibits performance to within 3 dB of the MF. The AMF performance operating in non-homogeneous training data with and without NHD pre-processing is carried out by Monte Carlo simulation at AFRL. For this example, the training data contained thirty high-amplitude, mainbeam discrete targets located at various range cells and Doppler frequencies. Initial sample support for NHD pre-processing is 6M. A sliding window approach is used to select a subset consisting of 4M training data realizations. Each GIP value obtained at a specific range cell is computed using $\hat{\mathbf{R}}$ formed from 2M adjacent training data vectors. Previously, we noted the sub-optimality of this scheme. In practice, its use is dictated by training data size limitations. In this manner 4M GIP values are obtained. The NHD pre-processing used in this example is based on a comparison of the empirical GIP with its theoretical mean value given by (3.7). The training data used in forming $\hat{\mathbf{R}}$ after NHD processing is obtained by sorting the GIP values and retaining $K = 2M$ realizations corresponding to the smallest GIP deviation from the theoretical mean of (3.7). Observe that the AMF performance in non-homogenous clutter degrades severely. Also note that NHD pre-processing restores the AMF performance to its analytical value. Figure 6.2 shows a plot of the GIP versus range prior to NHD pre-processing for the simulated data used in carrying out the performance analysis of Figure 6.1. Figure 6.3 shows a plot of the sorted absolute value of the difference between the GIP and its theoretical mean versus range after NHD pre-processing for the example in Figure 6.1. Observe the absence of discretes in the first $K = 2M$ range cells. Figure 6.4 depicts performance using measured data from the MCARM program [19]. For this case, it is not possible to present performance in terms of detection probability versus SINR. This is due to the fact that only one realization of target present data is available. Hence, we present a plot of the detection test statistic versus range. Since the AMF test statistic is an ad-hoc estimate of the output SINR, and since the probability of detection is a monotonically increasing function of the output SINR, this is an acceptable performance metric. Performance of the AMF without NHD processing degrades significantly in non-homogeneous clutter. Performance improvement is noted when the AMF is employed in non-homogeneous data with NHD pre-processing. Consequently, the use of NHD affords moderate performance improvement of the AMF test in non-homogeneous clutter. The performance with measured data is characterized by the ratio of the test statistic at the test cell to the mean of the test statistics formed from adjacent cells, Ψ_1 , and the ratio of the test statistic at the test cell to the highest test statistic formed from adjacent cells, Ψ_2 , respectively. Table 1 shows these values for the AMF test with and without NHD pre-processing.

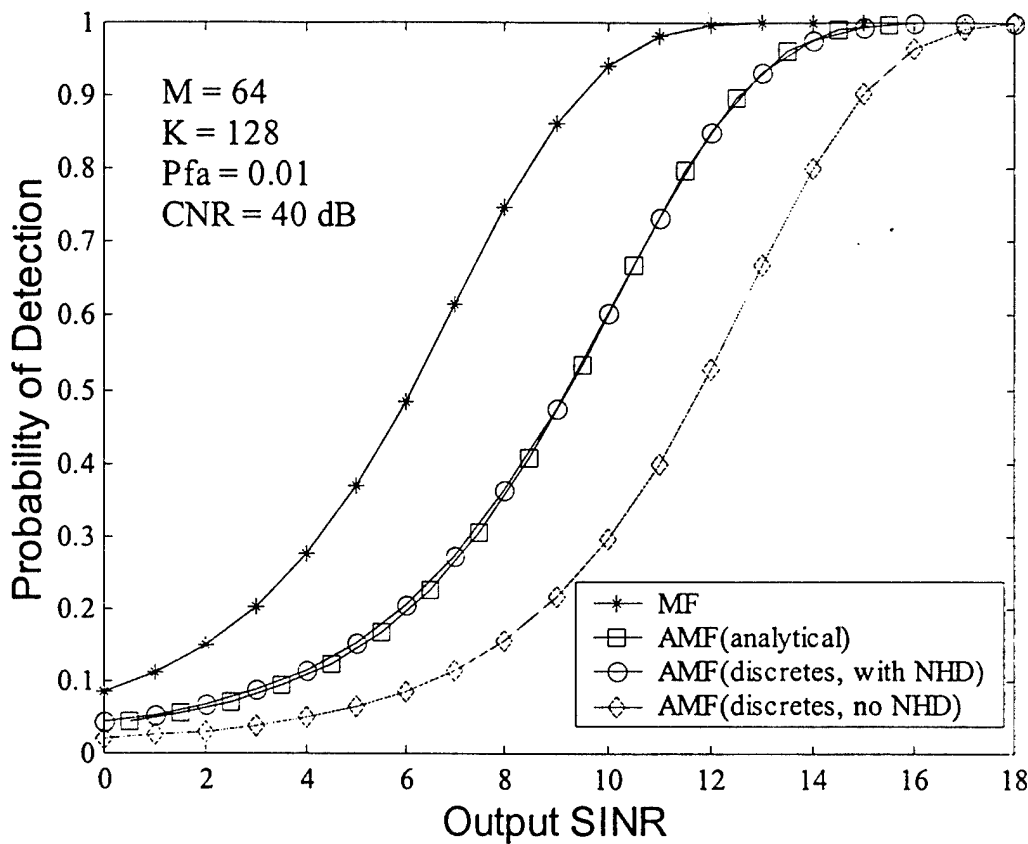


Figure 6.1: Performance of the AMF with and without NHD

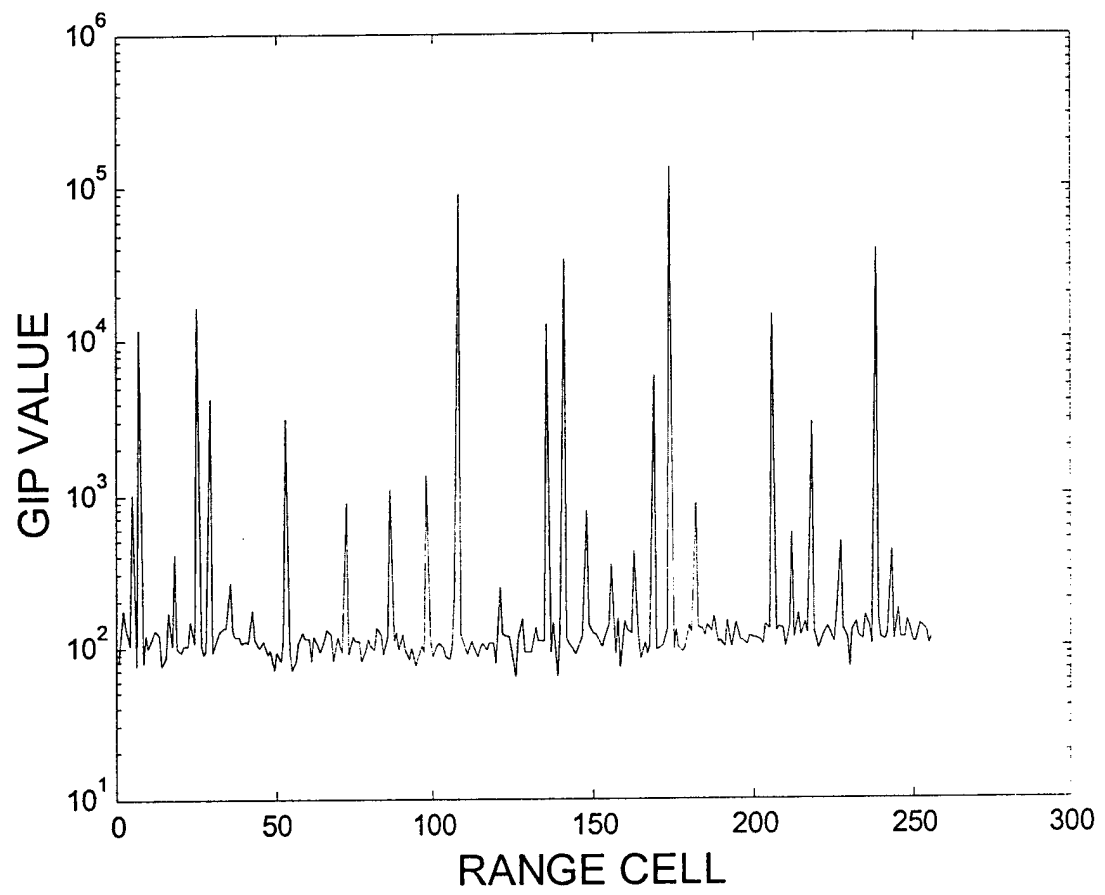


Figure 6.2: GIP versus Range

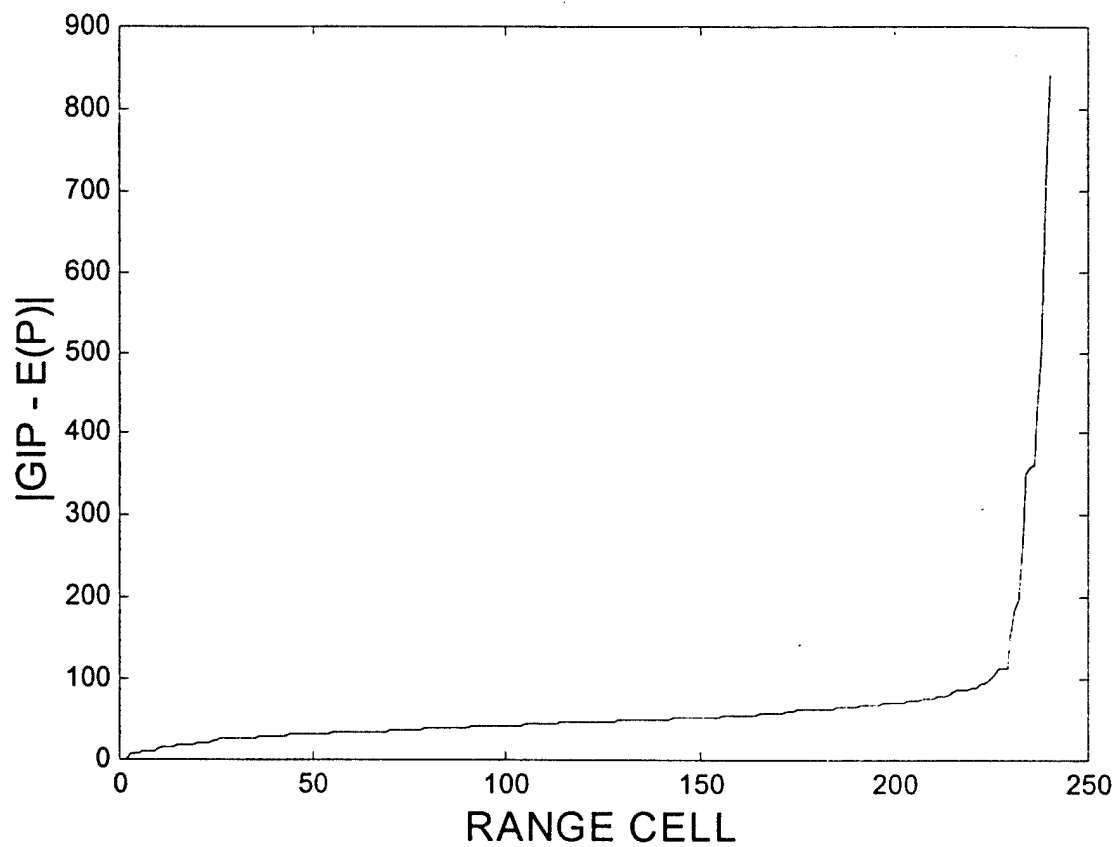


Figure 8: Absolute value of difference between GIP and Theoretical GIP mean vs Range

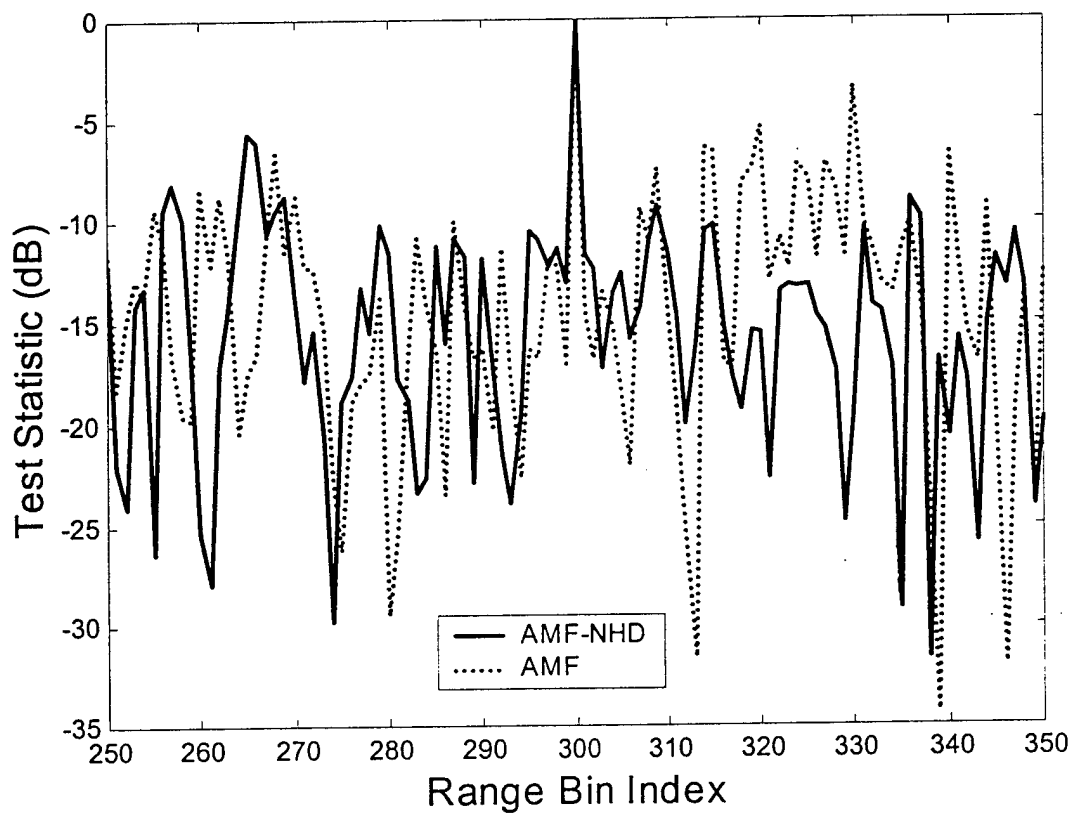


Figure 6.4: AMF Test Statistic vs Range

Algorithm	Ψ_1 (dB)	Ψ_2 (dB)
AMF with NHD	13.25	5.68
AMF without NHD	11.83	3.38

Table 6.1: AMF Performance with MCARM Data

Chapter 7

Conclusion

This report has made several significant contributions. First, we provided a statistical characterization of the GIP based NHD developed in [1–4,8]. We showed that the underlying GIP statistics deviate significantly when the unknown covariance matrix is estimated using finite sample support. We derived a canonical representation for the GIP in terms of two statistically independent random variables and showed that the normalized GIP follows a central-F distribution. These facts were then used to construct goodness-of-fit tests, whose performance is presented using both simulated and measured data. Application of this of this method as a pre-processing method for training data selection in the adaptive matched filter algorithm (AMF) was presented. Performance on the AMF in contaminated training data degrades significantly. The use of our pre-processing method for training data selection restores the AMF performance to within 3 dB of the optimal matched filter (MF) performance. This fact is illustrated with simulated as well as measured data from the MCARM program.

Bibliography

- [1] P. Chen, "On testing the equality of covariance matrices under singularity," tech. rep., for AFOSR Summer Faculty Research Program, Rome Laboratory, August 1994.
- [2] P. Chen, "Partitioning procedure in radar signal processing problems," tech. rep., for AFOSR Summer Faculty Research Program, Rome Laboratory, August 1995.
- [3] W. Melvin, M. Wicks, and R. Brown, "Assessment of multichannel airborne radar measurements for analysis and design of space-time adaptive processing architectures and algorithms," in *Proceedings of the IEEE National Radar Conference*, (Ann Arbor, MI), 1996.
- [4] W. Melvin and M. Wicks, "Improving practical space-time adaptive radar," in *Proceedings of the IEEE National Radar Conference*, (Syracuse, NY), 1997.
- [5] D. Rabideau and A. Steinhardt, "Improving the performance of adaptive arrays in nonstationary environments through data-adaptive training," in *Proceedings of the 30th Asilomar Conference on Signals, Systems, and Computers*, (Pacific Grove, CA), 1996.
- [6] D. Rabideau and A. Steinhardt, "Power selected training for false alarm mitigation in airborne radar," in *Proceedings of the Adaptive Sensor Array Processing Workshop (ASAP)*, (MIT Lincoln Laboratory, Lexington, MA), 1996.
- [7] D. Rabideau and A. Steinhardt, "Improved adaptive clutter cancellation through data-adaptive training," *IEEE Trans. on Aerospace and Electronic Systems*, vol. **AES-35**, no.3, pp. 879–891, 1999.
- [8] B. Himed, Y. Salama, and J. H. Michels, "Improved detection of close proximity targets using two-step NHD," in *Proceedings of the International Radar Conference*, (Alexandria, VA), 2000.
- [9] R. Nitzberg, "An effect of range-heterogenous clutter on adaptive Doppler filters," *IEEE Trans. on Aerospace and Electronic Systems*, vol. **26**, no.3, pp. 475–480, 1990.

- [10] W. L. Melvin, J. R. Guerci, M. J. Callahan, and M. C. Wicks, "Design of adaptive detection algorithms for surveillance radar," in *Proceedings of the International Radar Conference*, (Alexandria, VA), 2000.
- [11] W. L. Melvin, "Space-time adaptive radar performance in heterogenous clutter," *IEEE Trans. on Aerospace and Electronic Systems*, vol. **36**, no.2, pp. 621–633, 2000.
- [12] M. Rangaswamy, D. Weiner, and A. Ozturk, "Non-Gaussian random vector identification using spherically invariant random processes," *IEEE Trans. on Aerospace and Electronic Systems*, vol. **AES-29**, pp. 111–124, 1993.
- [13] P. Chen, W. Melvin, and M. Wicks, "Screening among multivariate normal data," *Journal of Multivariate Analysis*, vol. 69, pp. 10–29, 1999.
- [14] F. Robey, D. Fuhrmann, E. Kelly, and R. Nitzberg, "A CFAR adaptive matched filter detector," *IEEE Trans. on Aerospace and Electronic Systems*, vol. **AES-28**, pp. 208–216, 1992.
- [15] W. Chen and I. Reed, "A new CFAR detection test for radar," *Digital Signal Processing*, vol. **1**, pp. 198–214, 1991.
- [16] L. Cai and H. Wang, "On adaptive filtering with the CFAR feature and its performance sensitivity to non-Gaussian interference," in *Proceedings of the 24th Annual conference on Information Sciences and Systems*, (Princeton, NJ), pp. 558–563, 1990.
- [17] A. Papoulis, *Probability, Random Variables and Stochastic Processes*. New York: McGraw-Hill, 1991.
- [18] T. Anderson, *An introduction to multivariate statistical analysis*. New York: John Wiley and sons, 1958.
- [19] MCARMDATA, "View [www@http://128.132.2.229](http://128.132.2.229)." Data from the Multichannel Airborne Radar Measurement Program of the U.S. Air Force Research Laboratory, Rome, NY.
- [20] I. Reed, J. Mallett, and L. Brennan, "Rapid convergence rate in adaptive arrays," *IEEE Trans. on Aerospace and Electronic Systems*, vol. **AES-10**, pp. 853–863, 1974.

Appendix A: GIP PDF for Known Covariance Matrix

In this appendix, we show that for known \mathbf{R} , the GIP given by $Q = \mathbf{x}\mathbf{R}^{-1}\mathbf{x}$ follows a Chi-Squared distribution with M complex degrees of freedom and is given by (2.5).

We begin by noting that $\mathbf{w} = \mathbf{R}^{-\frac{1}{2}}\mathbf{x}$ is simply a linear transformation of a complex-Gaussian random vector. Consequently, \mathbf{w} is also a complex-Gaussian random vector. It follows that

$$\begin{aligned} E(\mathbf{w}) &= \mathbf{R}^{-\frac{1}{2}}E(\mathbf{x}) = \mathbf{0} \\ E(\mathbf{w}\mathbf{w}^H) &= \mathbf{R}^{-\frac{1}{2}}E(\mathbf{x}\mathbf{x}^H)\mathbf{R}^{-\frac{1}{2}} = \mathbf{I}. \end{aligned} \quad (\text{A.1})$$

Thus,

$$Q = \mathbf{x}\mathbf{R}^{-1}\mathbf{x} = \|\mathbf{w}\|^2 = \sum_{i=1}^M |W_i|^2 \quad (\text{A.2})$$

where W_i , $i = 1, 2, \dots, K$ are independent identically distributed $CN(0, 1)$ random variables. The PDF of W_i is given by

$$f_{W_i}(w_i) = \frac{1}{\pi} \exp(-|W_i|^2). \quad (\text{A.3})$$

Let $R_i = |W_i| = \sqrt{(W_{ci}^2 + W_{si}^2)}$ and $\Theta_i = \tan^{-1}(\frac{W_{si}}{W_{ci}})$, where W_{ci} and W_{si} denote the in phase and quadrature components of W_i . The Jacobian of the transformation is given by $J = \frac{1}{R_i}$. The joint PDF of R_i and θ_i is given by

$$f_{R_i, \Theta_i}(r_i, \theta_i) = \frac{1}{|J|} f_{W_i}(w_i) = \frac{r_i}{\pi} \exp(-r_i^2). \quad (\text{A.4})$$

Noting that

$$f_{R_i, \Theta_i}(r_i, \theta_i) = f_{R_i}(r_i) f_{\Theta_i}(\theta_i) \quad (\text{A.5})$$

where

$$\begin{aligned} f_{R_i}(r_i) &= 2r_i \exp(-r_i^2) \quad r_i \geq 0 \\ f_{\Theta_i}(\theta_i) &= \frac{1}{2\pi} \quad 0 \leq \theta_i \leq 2\pi. \end{aligned} \quad (\text{A.6})$$

Therefore, R_i and θ_i are statistically independent random variables. The characteristic function of R_i is given by

$$\Phi_{R_i^2}(\omega) = E[\exp(-j\omega R_i^2)] = \frac{1}{(1+j\omega)}. \quad (\text{A.7})$$

Recognizing that $Q = \mathbf{x}\mathbf{R}^{-1}\mathbf{x} = \|\mathbf{w}\|^2 = \sum_{i=1}^M |W_i|^2 = \sum_{i=1}^M R_i^2$, it follows that the characteristic function of Q can be expressed as

$$\Phi_Q(\omega) = E[\exp(-j\omega Q)] = \prod_{i=1}^M \Phi_{R_i^2}(\omega) = \frac{1}{(1+j\omega)^M}. \quad (\text{A.8})$$

Taking the inverse Fourier Transform of (A.8) yields the PDF of Q , which is given by

$$f_Q(q) = \frac{q^{M-1}}{\Gamma(M)} \exp(-q) \quad q \geq 0. \quad (\text{A.9})$$

Appendix B: Stochastic Representation for the Normalized GIP

Let \mathbf{Z} denote a data matrix whose columns are the previously defined \mathbf{z}_i , $i = 1, 2, \dots, K$. The maximum likelihood estimate of the covariance matrix is then expressed as $\hat{\mathbf{R}} = \frac{1}{K} \mathbf{S}_z$, where $\mathbf{S}_z = \mathbf{Z}\mathbf{Z}^H$. Consequently, the normalized GIP is expressed as

$$P' = \mathbf{x}^H \mathbf{S}_z^{-1} \mathbf{x}. \quad (\text{B.1})$$

The data matrix \mathbf{Z} and the vector \mathbf{x} admit a statistical representation of the form

$$\begin{aligned} \mathbf{Z} &= \mathbf{R}^{\frac{1}{2}} \mathbf{Y} \\ \mathbf{x} &= \mathbf{R}^{\frac{1}{2}} \mathbf{y} \end{aligned} \quad (\text{B.2})$$

where \mathbf{Y} is a data matrix whose columns, \mathbf{y}_i , $i = 1, 2, \dots, K$ are iid $\mathcal{CN}(0, \mathbf{I})$ random vectors and \mathbf{y} is a $\mathcal{CN}(0, \mathbf{I})$ random vector, which is statistically independent of \mathbf{Y} . Hence, the normalized GIP is expressed as

$$P' = \mathbf{y}^H \mathbf{S}_y^{-1} \mathbf{y} \quad (\text{B.3})$$

where $\mathbf{S}_y = \mathbf{Y}\mathbf{Y}^H$. Next, we use a Householder transformation defined by $\mathbf{A} = \mathbf{I} - 2 \frac{\mathbf{u}\mathbf{u}^H}{\mathbf{u}^H \mathbf{u}}$, where $\mathbf{u} = \mathbf{y} - \|\mathbf{y}\| \mathbf{e}$ and $\mathbf{e} = [1 \ 0 \ 0 \ \dots \ 0]^T$, so that $\tilde{\mathbf{y}} = \mathbf{A}\mathbf{y} = \|\mathbf{y}\| \mathbf{e}$. Also, let $\tilde{\mathbf{Y}} = \mathbf{A}\mathbf{Y}$. Since $\mathbf{A} = \mathbf{A}^H$ and $\mathbf{A}\mathbf{A}^H = \mathbf{A}^H \mathbf{A} = \mathbf{I}$, it follows that the statistics of $\tilde{\mathbf{Y}}$ are identical to that of \mathbf{Y} . Consequently, the normalized GIP is expressed as

$$P' = \tilde{\mathbf{y}}^H \mathbf{S}_{\tilde{y}}^{-1} \tilde{\mathbf{y}} \quad (\text{B.4})$$

where $\mathbf{S}_{\tilde{y}} = \tilde{\mathbf{Y}}\tilde{\mathbf{Y}}^H$. Furthermore, we partition $\tilde{\mathbf{Y}}$ as

$$\tilde{\mathbf{Y}} = \begin{bmatrix} \tilde{\mathbf{y}}_1^H \\ \tilde{\mathbf{Y}}_{11}^H \end{bmatrix} \quad (\text{B.5})$$

where $\tilde{\mathbf{y}}_1^H$ is the first row of $\tilde{\mathbf{Y}}$ and $\tilde{\mathbf{Y}}_{11}^H$ denotes the $(M - 1) \times K$ matrix formed from the remaining rows of $\tilde{\mathbf{Y}}$. Consequently, $\mathbf{S}_{\tilde{\mathbf{y}}}$ is expressed as

$$\mathbf{S}_{\tilde{\mathbf{y}}} = \begin{bmatrix} \tilde{\mathbf{y}}_1^H \tilde{\mathbf{y}}_1 & \tilde{\mathbf{y}}_1^H \tilde{\mathbf{Y}}_{11} \\ \tilde{\mathbf{Y}}_{11}^H \tilde{\mathbf{y}}_1 & \tilde{\mathbf{Y}}_{11}^H \tilde{\mathbf{Y}}_{11} \end{bmatrix}. \quad (\text{B.6})$$

The inverse of $\mathbf{S}_{\tilde{\mathbf{y}}}$ admits a representation of the form

$$\mathbf{S}_{\tilde{\mathbf{y}}}^{-1} = \begin{bmatrix} \mathbf{S}^{11} & \mathbf{S}^{12} \\ \mathbf{S}^{21} & \mathbf{S}^{22} \end{bmatrix} \quad (\text{B.7})$$

Finally, the normalized GIP is expressed as

$$P' = \|\mathbf{y}\|^2 \mathbf{S}^{11}. \quad (\text{B.8})$$

However, from the matrix inversion Lemma it follows that $\mathbf{S}^{11} = [\tilde{\mathbf{y}}_1^H \mathbf{P}_\perp \tilde{\mathbf{y}}_1]^{-1}$, where $\mathbf{P}_\perp = [\mathbf{I} - \tilde{\mathbf{Y}}_{11}(\tilde{\mathbf{Y}}_{11}^H \tilde{\mathbf{Y}}_{11})^{-1} \tilde{\mathbf{Y}}_{11}^H]$. Since $\tilde{\mathbf{Y}}_{11}(\tilde{\mathbf{Y}}_{11}^H \tilde{\mathbf{Y}}_{11})^{-1} \tilde{\mathbf{Y}}_{11}^H$ is a projection matrix of rank $M-1$, it follows that \mathbf{P}_\perp is a projection matrix of rank $K-M+1$. Consequently, $\tilde{\mathbf{y}}_1^H \mathbf{P}_\perp \tilde{\mathbf{y}}_1 = \sum_{i=1}^{K-M+1} |\tilde{y}_1(i)|^2$. Therefore, \mathbf{S}^{11} is simply the reciprocal of a chi-squared distributed random variable with $K - M + 1$ complex degrees of freedom. Also, $\|\mathbf{y}\|^2$ is simply the sum of the squared magnitudes of M iid $\text{CN}(0,1)$ random variables and hence follows a chi-squared distribution with M complex degrees of freedom. Consequently, the GIP admits a representation of the form of (3.2).

Statistical Analysis of the Non-homogeneity Detector for STAP Applications

Muralidhar Rangaswamy
AFRL/SNHE
80 Scott Drive
Hanscom AFB, MA 01731

Braham Himed
AFRL/SNRT
26 Electronic Parkway
Rome, NY 13441

James H. Michels
AFRL/SNRT
26 Electronic Parkway
Rome, NY 13441

Abstract — We present a statistical analysis of the recently proposed non-homogeneity detector (NHD) for Gaussian interference statistics. We show that a formal goodness-of-fit test can be constructed by accounting for the statistics of the generalized inner product (GIP) used as the NHD test statistic. Specifically, the Normalized-GIP is shown to follow a central-F distribution and admits a canonical representation in terms of two statistically independent Chi-squared distributed random variables. Moments of the GIP can be readily calculated as a result. These facts are used to derive the goodness-of-fit tests, which facilitate intelligent training data selection. Additionally, we address the issue of space-time adaptive processing (STAP) algorithm performance using the NHD as a pre-processing step for training data selection. Performance results are reported using simulated as well as measured data.

I. INTRODUCTION

An important issue in space-time adaptive processing (STAP) for radar target detection is the formation and inversion of the covariance matrix underlying the clutter and interference. Typically, the unknown interference covariance matrix is estimated from a set of independent identically distributed (iid) target-free training data that is representative of the interference statistics in a cell under test. Frequently, the training data is subject to contamination by discrete scatterers or interfering targets. In either event, the training data becomes non-homogeneous. Consequently, it is not representative of the interference in the test cell. Estimates of the covariance matrix from non-homogeneous training data result in severely under-nulled clutter. Consequently, CFAR and detection performance suffer. Significant performance improvement can be achieved by employing pre-processing to select representative training data.

The problem of target detection using improved training strategies has been considered in [1-8]. The impact of non-homogeneity on STAP performance is considered in [9-11]. It was shown in [12] that the distribution information of a class of multivariate probability density functions (PDF) is succinctly determined through an equivalent univariate PDF of a quadratic form. An application of this result is the non-homogeneity detector (NHD) based on the generalized inner product (GIP) [1-4,8].

Non-homogeneity of the training data arises due to a number of factors such as contaminating targets, presence of strong discretes, and non-stationary reflectivity properties of the scattering surface. In these scenarios, the test cell disturbance covariance matrix, \mathbf{R}_T , differs significantly from the estimated covariance matrix, $\hat{\mathbf{R}}$ formed using target-free disturbance realizations from adjacent reference cells [13]. If a large number of test cell data realizations are available, the underlying non-homogeneity is characterized via the eigenvalues of $\hat{\mathbf{R}}^{-1}\mathbf{R}_T$ [14]. However, in radar applications, only a single realization of test cell data is usually available. Consequently, the resulting estimate of \mathbf{R}_T is singular. Hence, [1-4,8] compared the empirically formed GIP with a theoretical mean corresponding to a ‘known’ covariance matrix. Large deviations of the GIP mean from the theoretical mean have been ascribed to non-homogeneity of the training data. Such an approach provides meaningful results in the limit of large training data size. In practice, the amount of training data available for a given application is limited by

Douglas M. Richards
THIS MATERIAL HAS BEEN CLEARED
FOR PUBLIC RELEASE BY ESC/PA

19 Nov 01

ESC 01 - 1438